Electronic Journal of Biotechnology 40 (2019) 30–39

Contents lists available at ScienceDirect

Electronic Journal of Biotechnology

Research Article

CRISPR/Cas9-mediated *MSTN* gene editing induced mitochondrial alterations in C2C12 myoblast cells

Lamei Wang [1], Sen Ma [1], Qiang Ding, Xiaolong Wang, Yulin Chen *

College of Animal Science and Technology, Northwest A&F University, Yangling 712100, China

ARTICLE INFO

Article history:
Received 11 September 2018
Accepted 29 March 2019
Available online 5 April 2019

Keywords:
CRISPR/Cas9
Differentiation
Genome-editing
Intracellular organelles
Metabolism regulation
Mitochondria biogenesis
Mitochondria metabolism
Myostatin
Proliferation
Short RNAs
Skeletal muscle

ABSTRACT

Background: Myostatin (MSTN) negatively regulates muscle mass and is a potent regulator of energy metabolism. However, MSTN knockout have affect mitochondrial function. This research assessed the mitochondrial energy metabolism of Mstn −/+ KO cells, and wondered whether the mitochondria biogenesis are affected.
Results: In this study, we successfully achieved Mstn knockout in skeletal muscle C2C12 cells using a CRISPR/Cas9 system and measured proliferation and differentiation using the Cell-Counting Kit-8 assay and qPCR, respectively. We found that MSTN dysfunction could promote proliferation and differentiation compared with the behaviour of wild-type cells. Moreover, Mstn KO induced an increase in KIF5B expression. The mitochondrial content was significantly increased in Mstn KO C2C12 cells, apparently associated with the increases in PGC-1α, Cox1, Cox2, ND1 and ND2 expression. However, no differences were observed in glucose consumption and lactate production. Interestingly, Mstn KO C2C12 cells showed an increase in IL6 and a decrease in TNF-1α levels.
Conclusion: These findings indicate that MSTN regulates mitochondrial biogenesis and metabolism. This gene-editing cells provided favourable evidence for animal breeding and metabolic diseases.
How to cite: Wang L, Ding Q, Ma S, et al. CRISPR/Cas9-mediated *MSTN* gene editing Induced Mitochondrial Alterations in C2C12 myoblast Cells. Electron J Biotechnol 2019;40. https://doi.org/10.1016/j.ejbt.2019.03.009

1. Introduction

The clustered regularly interspaced short palindromic repeats (CRISPR)/CRISPR associated 9 protein (Cas9) adaptive immune systems found in bacteria can be directed by short RNAs to induce precise DNA cleavage [1]. The CRISPR/Cas9 genome-editing tool offers a promising route for genetic engineering due to its simple design and high efficacy in many species, including zebrafish [2], mouse [3], monkeys [4], pigs [5] and goats [6].

Myostatin, also known as growth and differentiation factor 8 (GDF8), is a member of the TGF-β family primarily expressed in skeletal muscle. MSTN is a negative regulator of skeletal muscle mass, myostatin dysfunction can significant increase in skeletal muscle mass [7]. *Mstn* gene mutations have been linked with the double-muscle phenotype in Belgian Blue and Piedmontese cattle, resulting in the skeletal muscle mass were marked increase compared to that of wild type normal cattle [8].

Alterations in mitochondrial function, as have been associated with oxidative stress [9], metabolic, degenerative and autoimmune disease [10], as well as disruption of the structure and function of lysosomes, the main organelle responsible for degradation and recycling [11]. Mitochondria, as the main and most efficient producers of cellular ATP and of the metabolites necessary for the bioenergetics and biosynthetic demands of the cell, have a herculean task to fulfil [12]. ATP provides the chemical energy to fuel vital cellular processes. Skeletal muscle plays a vital role in the body. Two intracellular organelles, Ca^{2+} release units [13] and mitochondria [14] where Ca^{2+} and ATP come from, respectively, are extremely important and necessary for skeletal muscle contraction and endurance. Mitochondrial health is vital not only for efficacious energy provision but also for proper cellular signalling and homeostasis. Thus, mitochondrial abnormalities are often found in a variety of muscle wasting diseases [15], muscular dystrophies [16,17] and cachexia [18]. Ploquin et al. [19] reported that myostatin dysfunction leads to a decrease in mitochondrial content, a reduced expression of cytochrome *c* oxidase, and a lower citrate synthase activity in skeletal muscle in $Mstn^{-/-}$ KO mice compared with wild-type (WT) mice. However, Girgenrath et al. [20] reported that myostatin inhibition may alter the skeletal muscle fibre composition in *Mstn*-null mice than in their wild-type littermates, as shown in the

* Corresponding author.
E-mail address: chenyulin@nwafu.edu.cn (Y. Chen).
[1] These authors contributed equally to this work.
Peer review under responsibility of Pontificia Universidad Católica de Valparaíso.

https://doi.org/10.1016/j.ejbt.2019.03.009

higher proportion of fast-twitch fibres in the soleus and extensor digitorum longus muscles. Disruptions in the *Mstn* gene have been reported to be associated with distance racing, skeletal muscle fibre composition and body composition in horses [21]. More interestingly, Wang et al. [22] have reported *Mstn* to be associated with mitochondrial metabolism by transcriptomics analysis. Altered metabolism of mitochondria were carried out investigate by a comparative proteomic in the gastrocnemius muscle of *Mstn*-null mice compared with wild-type mice. A sequence similar to that of the aldehyde reductase was increased in the *Mstn*-null mitochondria [23]. In this context, we wanted to assess the mitochondrial energy metabolism of $Mstn^{-/+}$ KO cells in animals, and wondered whether the mitochondria are affected.

Improved mitochondrial performance plays a vital role in animal breeding and protecting the body against obesity. In this study, we established stable C2C12 cell lines in which *Mstn* was knocked out. We applied RT-qPCR, Western blot, flow cytometry, mtDNA copy number and mitochondrial membrane potential techniques to investigate the effects of *Mstn* KO on cellular mitochondrial biogenesis and energy metabolism. We demonstrate that *Mstn* KO enhances mitochondrial biogenesis and alters energy metabolism in C2C12 cells.

2. Materials and methods

2.1. Cell culture

Skeletal muscle C2C12 mouse myoblasts were obtained from the Cell Bank of the Chinese Academy of Sciences (Shanghai, China) and maintained in DMEM/F12 medium containing 10% foetal bovine serum (FBS) in 5% CO_2 at 37°C. When the cells reached confluence, the serum in the medium was changed to 2% heat-inactivated horse serum with 100-U/mL penicillin and 100-μg/mL streptomycin to promote differentiation for 7 d. The medium was replaced every two days.

2.2. Design and preparation of sgRNA

High-quality guide RNA with minimum off-targets and a high quality score (99) was designed using the CRISPR design tool (http://crispr.mit.edu). Targeting sgRNA1 and sgRNA2 for all the exons of the *Mstn* genomic region were designed. The CRISPR/Cas9 target sequences twenty base pairs directly upstream of any 5′-NGG were identified and used in this study, shown in **Table S1**. The paired synthesised oligonucleotides for sgRNAs were annealed and sub-cloned into the pUC57-U6-sgRNA (Addgene #51132) expression vector. The resulting expression vectors for sgRNA were confirmed by Sanger sequencing.

2.3. Plasmid transfection, T7 endonuclease I assay, sequencing analysis, and single-cell colony selection

The transfection procedure was carried out using Lipofectamine 3000 Reagent (Invitrogen, USA) according to the manufacturer's instructions. Approximately 1×10^6 C2C12 cells were transfected with *Mstn* pUC57-U6-sgRNA1 (1.5 μg) and *Mstn* pUC57-U6-sgRNA2 (1.5 μg) along with 1 μg of Cas9 plasmid using Lipofectamine 3000 in a 6-well culture plate. Twenty-four hours after transfection, 7 mg/mL of puromycin and 21 mg/mL of blasticidine S hydrochloride were added to the medium and incubated for approximately 10 d.

To determine the cutting efficacy, genomic DNA from surviving colonies was extracted using the Universal Genomic DNA Kit (CWBIO, China), and the regions surrounding the target sites were amplified by PCR. A T7EI cleavage assay was carried out as described by Shen et al. [24]. Briefly, the targeted fragments were amplified with KOD DNA polymerase (Toyobo, Japan) from the genomic DNA and purified with a Cycle Pure Kit (OMEGA, China) according to the manufacturer's instructions. The primers for the amplification of the *Mstn*-targeted fragments are listed in **Table S1**. The hybridization reaction contained 200 ng of purified PCR product in NEB buffer and was performed at 95°C for 10 min and at room temperature overnight. Five units of T7EI were added to digest the re-annealed DNA at 37°C for 20 min. The DNA fragment was separated by 2% agarose gel. The DNA band intensity was quantitated using Image Lab (Bio-Rad, USA). Positive single-cell colonies were used as donors for further study.

2.4. RNA isolation and gene expression analysis

Total cellular RNA was extracted from cell monolayers with an RNA Extraction Kit (Promega, Beijing, China) according to the manufacturer's instructions. The RNA was transcribed into cDNA using an Invitrogen SuperScript™ One-step RT-PCR Kit. A qRT-PCR assay was performed with SYBR Premix Ex Taq II (Takara, China) and monitored with a CFX96 Touch Real-time PCR Detection System (Bio-Rad, USA). GAPDH served as an endogenous control. All the primer sequences used in this assay are shown in Supplementary Information **Table S2.** Data were analysed using the $2^{-\Delta\Delta CT}$ method.

2.5. Immunoblotting

Cellular proteins were lysed on ice with RIPA assay buffer (Beyotime, China) along with PMSF (0.1 ~ 1 mM). Protein concentrations were determined with an Enhanced BCA Protein Assay Kit (Solarbio, China). The supernatants were resolved by SDS-PAGE (Invitrogen) and transferred to a PVDF membrane (Millipore), which was subsequently blocked with dry milk and incubated overnight with anti-GDF8 (Santa Cruz, CA, 1:200), anti-GLUT4 (Bioss, China, 1: 500), anti-FASN (Bioss, China, 1:500), and anti-cytochrome *C* (Bioss, China, 1:500) primary antibodies at 4°C. After washing three times, the membranes were incubated at room temperature for 1–2 h with horseradish peroxidase (HRP)-conjugated goat anti-rabbit IgG or mouse IgGκ binding protein-HRP (Santa Cruz, USA). Immunoreactive bands were detected with ECL reagent (Thermo Scientific, USA) and quantified using Quantity One. The results were normalised against β-actin (Beyotime, China).

2.6. Proliferation assay

The cell proliferation rate was determined using Cell-Counting Kit-8 (CCK8) (Beyotime, China) according to the manufacturer's instructions. C2C12 cells were seeded in 96-well plates at a density of 2×10^3/well in 100 μL of culture medium. Skeletal muscle cells were serum-starved in DMEM/F12 in 96-well plates for 12 h. The medium was removed, and the cells were further incubated for 24, 48, 72 and 96 h in DMEM/F12 with 10% FBS and then at 37°C in a 5% CO_2 incubator. The cell proliferation assay was performed by adding 10 μL of the CCK8 reagent to each well of the plate for 2 h. Cell density was determined by measuring the absorbance of the coloured formazan reaction product at OD450 nm using a microplate reader (Synergy H1, USA).

2.7. Glucose uptake assays

C2C12 myoblasts in 96-well plates were serum-starved for 12 h. After discarding and replacing the culture media with fresh media, its glucose concentration was determined with a Glucose Assay Kit (Sigma, USA) according to the manufacturer's instructions. The cells were then incubated for 1, 2, and 3 d, and the culture media were collected to measure the glucose concentration. The amount of glucose consumption was calculated as the difference between the initial concentration and the remaining glucose at a given time after correction for the change in glucose concentration in blank wells. Triplicate plates were analysed, and the test was repeated 3 times.

2.8. Mitochondrial DNA (mtDNA) copy number

Total genomic DNA was extracted from C2C12 cells using the Universal Genomic DNA Kit. qRT-PCR detection were performed using the CFX96 Touch Real-time PCR Detection System and ratio of mtDNA/nucleic DNA was calculated by normalising the mitochondrial gene mND1 to the nuclear gene cyclophilin A. qRT-PCR was carried out for mtDNA content in a 20-μL reaction containing 1X SYBR Green mixture with 100 ng of genomic DNA, as previously described [25,26].

2.9. Microscopy and image analysis

To assess the impact of *Mstn* gene on the morphology and dynamics of mitochondrial, skeletal muscle C2C12 cells cultures at 5-d post-culture, for mitochondrial staining, cells were stained with MitoTracker Red CMXRos (Ex: 490 nm; Em: 516 nm; final concentration, 100 nM), and MitoTracker green (Ex: 490 nm; Em: 516 nm; final concentration, 100 nM) containing fresh culture medium was then incubated with the cells for 40 min at 37°C in the dark. Mito-Tracker Green dyeing liquid was removed; cells cultured were incubated in fresh medium after the staining. The cells were then analysed under fluorescence microscopy (Leica DMI8). Images were processed using Adobe Photoshop CC 2018.

2.10. Determination of intracellular ATP content

Control group C2C12 and MSTN dysfunction cells grown to the proliferation phase (4 d) and differentiation phase (0, 2, 4, 6 and 8 d) were collected by centrifugation and washed with cold phosphate-buffered saline (PBS) buffer. ATP measurements were conducted using an Enhanced ATP Assay Kit (Beyotime, China) according to the manufacturer's instructions. Triplicate plates were analysed, and the test was repeated 3 times. Luminescence for ATP measurement was recorded with a Bio-Tek Synergy 2 automatic microplate reader. The concentration of ATP in each sample was calculated against the ATP calibration curve, and the results are shown in arbitrary units.

2.11. Flow cytometry

The total mitochondrial membrane potential was measured by incubating cells with the fluorescent probe JC-1 (5,5′,6,6-tetrachloro-1, 1′,3,3′-tetraethylbenzimidazolcarbocyanine iodide) (Nanjing, China). Briefly, 2 μg/mL of JC-1 was used to stain C2C12 cells for 20 min at 37°C and washed twice with PBS. Fluorescence was detected at 525/590 nm for JC-1 aggregates and at 480/530 nm for JC-1 monomers with a Partec CyFlow Cube Flow Cytometer running FlowJo. To measure reactive oxygen species (ROS), C2C12 myoblast cells were incubated with 10-μM 2,7-dichlorofluorescin diacetate (DCFH-DA) (Molecular Probes, China) for 1 h according to the manufacturer's instructions, after which fluorescence was measured using a Bio-Tek Synergy Neio HTS microplate reader.

2.12. Measurement of lactate production

Skeletal muscle C2C12 myoblast cells were seeded in 6-well plates, serum-starved for 12 h, and then serum-free medium was replaced with fresh growth medium. Following the incubation period, the medium was collected at 24, 48 and 72 h for determination of lactate. The total lactate released in the medium was measured using a Lactate Assay Kit (Cayman, USA) according to the manufacturer's instructions. Triplicate plates were analysed, and the test was repeated 3 times.

2.13. Statistical analysis

The mean of triplicate sample was calculated and used for further analysis. There were three independent samples for either control group

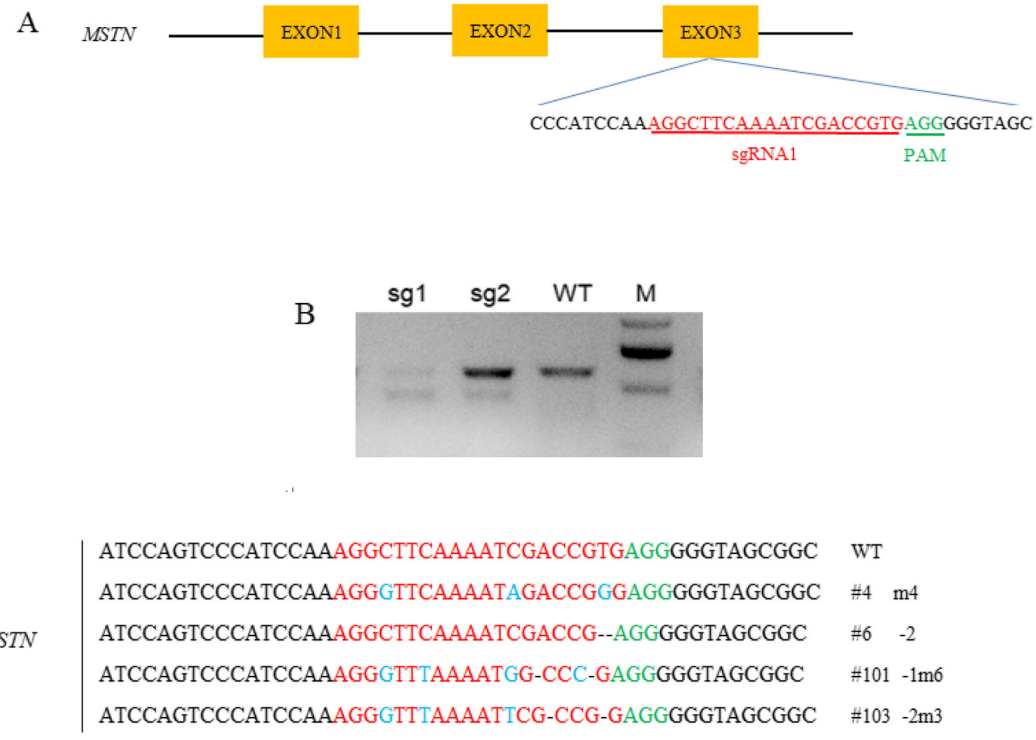

Fig. 1. Detection of the CRISPR/Cas9-mediated *Mstn* editing in C2C12 cells. (A) Schematic diagram of sgRNA targeting the mouse *Mstn* gene locus. (B) Mutation detection in C2C12 cells by T7EI cleavage assay. (C) Sequences of modified *Mstn* alleles. Numbers 4, 6, 101 and 103 represent different *Mstn* KO cell clones. M, marked; WT, wild-type PCR products from C2C12 cells not treated with CRISPR/Cas9. Target sequences complementary to *Mstn* sgRNA are shown in red and the mutations in blue. Deletions (−), mutation (m) or translocation (t) are shown to the right of each allele.

cells or *Mstn* KO cells at each analysis. Statistical comparisons of the empty vector C2C12 cell lines and the *Mstn* KO cell lines were analysed by two-tailed nonpaired *t*-tests. Data are expressed as mean ± SEM. Two-tailed $p < 0.05$ was considered statistically significant.

3. Results

3.1. Efficient generation of CRISPR/Cas9-mediated Mstn knockout in C2C12 myoblasts

Mammalian myostatin protein consists of a noncovalently held complex of the N-terminal propeptide and a disulphide-linked dimer of C-terminal fragments. Mutations in exon 3 of myostatin in mice and cattle can lead to increased muscle mass [7,27], which indicates the functional importance of this exon. Therefore, to knock out the *Mstn* gene in skeletal muscle cells, sgRNA1 and sgRNA2 were used to target the exon 3 region of *Mstn* based on the N20NGG rule [7] (Fig. 1A). The T7EI mutation detection assay was performed to detect the mutational efficacy of *Mstn*. The PCR products from wild-type C2C12 myoblasts showed one distinct band (725 bp), while those from *Mstn* KO myoblast cells showed two or more bands (<725 bp). Types of mutation were determined depended on various banding patterns by gel electrophoresis (Fig. 1B). Because the efficacy of *Mstn* KO by sgRNA1 was much higher than that achieved by *Mstn* sgRNA2, we chose *Mstn* sgRNA1 KO cells for Sanger sequencing. Because the cleavage was confirmed by Sanger sequencing, the observed indels at the target sites of *Mstn* with a range of mutation sizes are shown in Fig. 1C. The *Mstn*-sgRNA CRISPR/Cas9 system successfully induced frameshift mutations in exon 3 of the C2C12 myoblast *Mstn* genome.

We found significant differences in cell size and shape between *Mstn* KO and control cells (Fig. 2A). We found lower expression levels of the *Mstn* gene in *Mstn* KO C2C12 myoblasts than in control cells (Fig. 2B). Consistent with the qPCR analysis, Western blotting showed lower levels of *Mstn* protein in *Mstn* KO cells than in wild-type cells (Fig. 2C).

3.2. Mstn KO increases proliferation, differentiation and mitochondrial biogenesis in C2C12 myoblasts

To investigate the effects of *Mstn* KO on the proliferation of C2C12 myoblast cells, we compared the proliferation capability of the *Mstn* KO cells to that of the control group using a CCK8 Assay Kit. As shown in Fig. 3A, *Mstn* KO cells showed a significant increase in proliferation compared to the control group cells. After 0, 2, 4, 6, and 8 d of incubation of C2C12 cells in DMEM/F12 medium with 2% horse serum, the expression levels of *Mstn* associated with differentiation and mitochondrial biogenesis, such as KIF5B, PGC-1α and ND1, were typically increased in *Mstn* KO cells compared to control group cells (Fig. 3 B).

Basal mitochondrial content was marked increased in *Mstn* KO C2C12 cells, as evidenced by the expression levels of Cox1, Cox2, ND1 and ND2 (Fig. 3C). Meanwhile, mitochondria are composed of various proteins, including PGC-1α and cytochrome *c* oxidase subunits (COX2). Cytochrome *c* is encoded by nuclear genome, and plays an important role in mitochondrial electron transport chain. Western blotting revealed that PGC-1α and COX2 were upregulated in *Mstn* KO C2C12 cells as an evidence of increased mitochondrial biogenesis (Fig. 3D); furthermore, the mitochondrial DNA copy number was significantly increased (Fig. 3E). To further validate the suggestion that

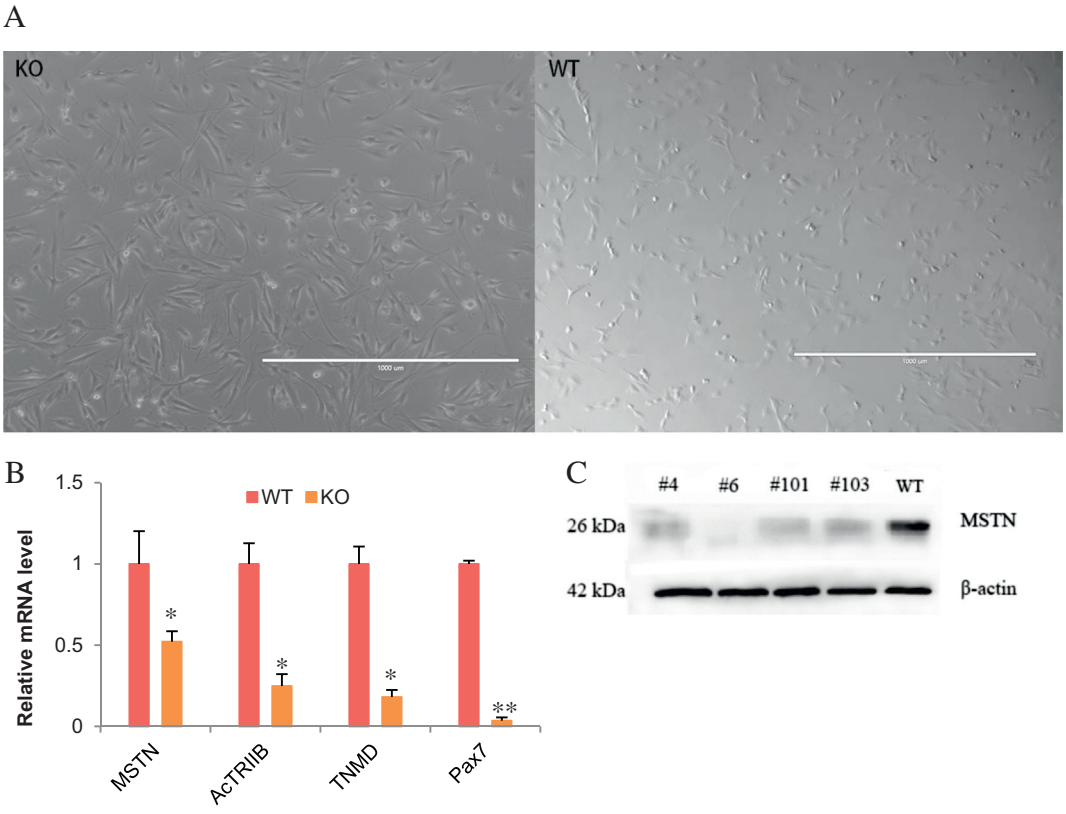

Fig. 2. Effects of *Mstn* KO on muscle development-related genes and Western blot analysis in C2C12 myoblasts. (A) Electron micrograph of *Mstn* KO and wild type C2C12 cells. (B) Relative mRNA expression of genes associated with muscle development in the liver was measured by qRT-PCR. The expression of muscle development-related genes was examined by qPCR in *Mstn* KO C2C12 myotubes. WT: wild type; KO: #6 cell clone. (C) Western blot of cell lysates with myostatin antibodies. β-actin served as a loading control. WT: wild type; Numbers 4, 6, 101 and 103 represent different *Mstn* KO cell clones. *$P < 0.05$; **$P < 0.01$ compared with empty vector control.

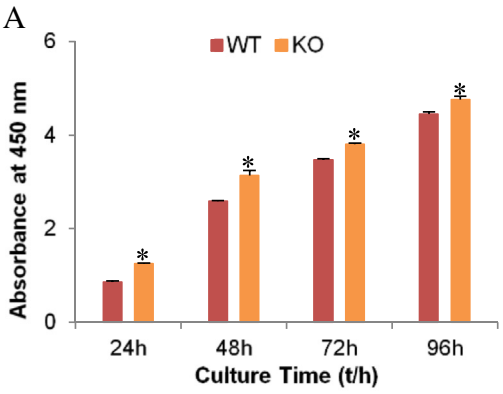
A
WT
KO
Absorbance at 450 nm
0
2
4
6
24h
48h
72h
96h
Culture Time (t/h)

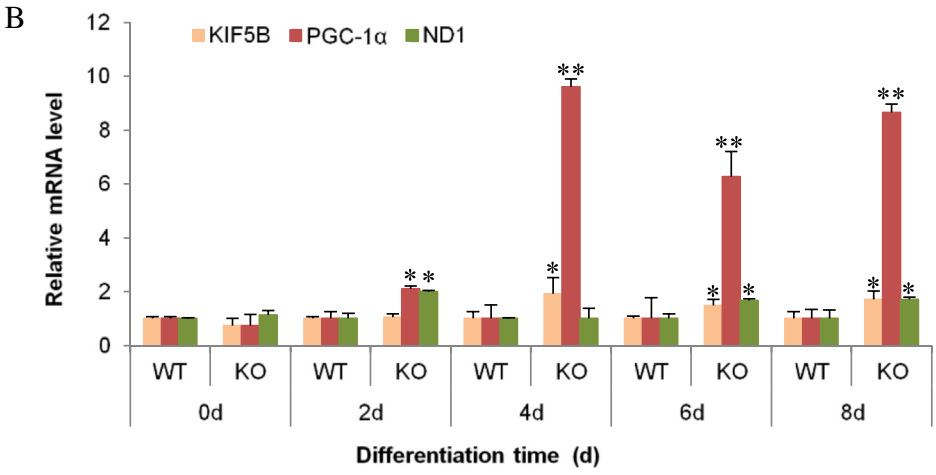
B
KIF5B
PGC-1α
ND1
Relative mRNA level
0
2
4
6
8
10
12
WT
KO
0d
2d
4d
6d
8d
Differentiation time (d)

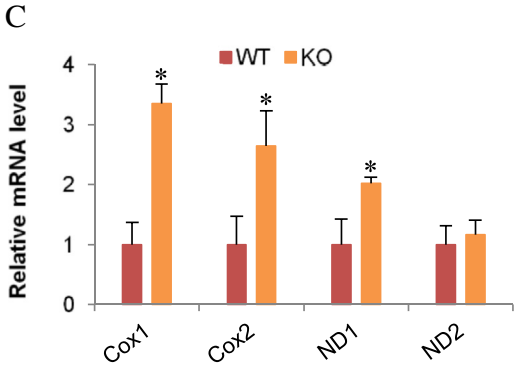
C
WT
KO
Relative mRNA level
0
1
2
3
4
Cox1
Cox2
ND1
ND2

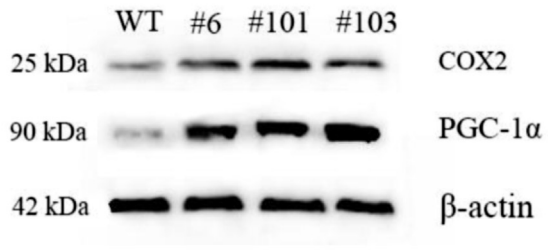
D
WT
#6
#101
#103
25 kDa
COX2
90 kDa
PGC-1α
42 kDa
β-actin

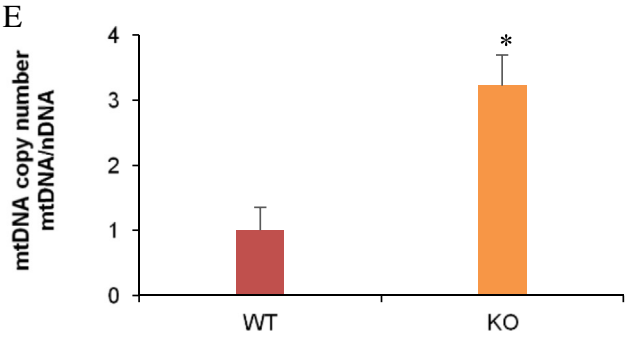
E
mtDNA copy number
mtDNA/nDNA
0
1
2
3
4
WT
KO

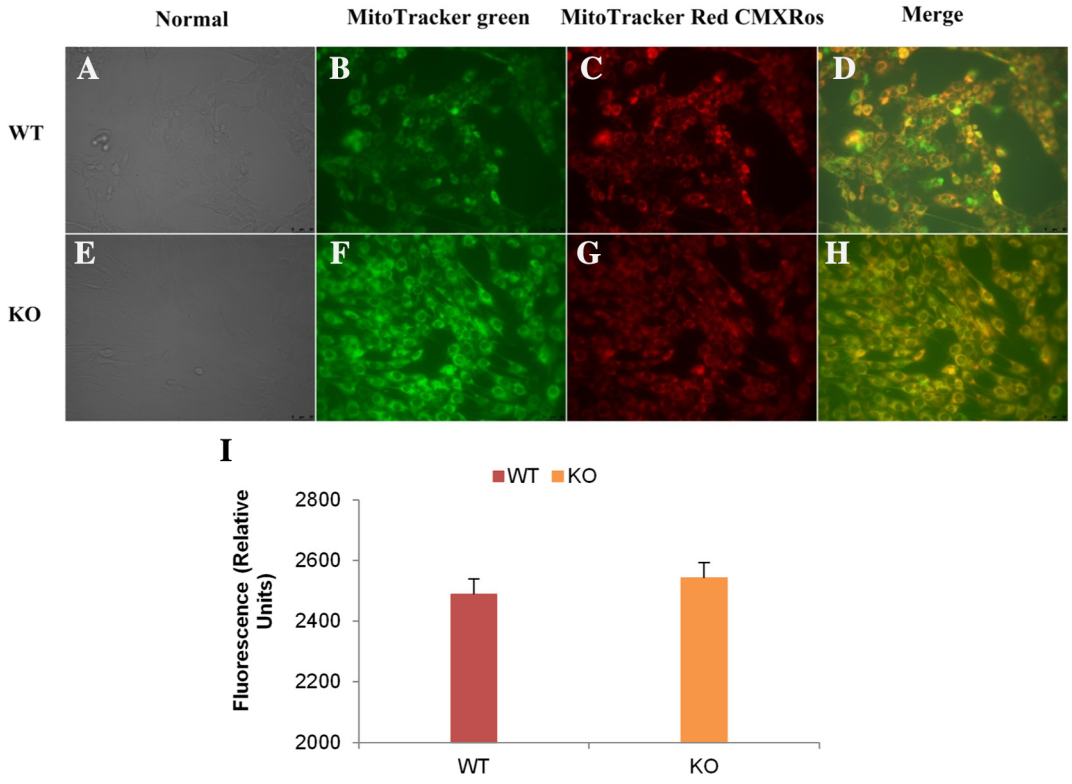

Fig. 4. *MSTN* knockout change mitochondrial morphology and dynamics in C2C12 cells by analysis of mitochondrial content by staining with MitoTracker Red and MitoTracker green. Wild type groups (A–D) and *MSTN* KO (E–H). ROS of cell Mitochondrial production (I). WT: wild type; KO: #6 cell clone.

mitochondrial mass is increased, mitochondrial of alive cells were measured by mitochondrial staining with MitoTracker green and MitoTracker CMXRos (Fig. 4). Meanwhile, ROS were further measured to prove MSTN dysfunction did not increase cellular mitochondrial product ROS, as shown in Fig. 4I. As expected, mitochondrial biogenesis was increased by *Mstn* KO in C2C12 cells. However, these results are shown that *Mstn* KO did not increase ROS production.

3.3. Mstn KO induces energy metabolism alterations in C2C12 myoblasts

We set out to assess the role of *Mstn* KO in the transcriptional regulation of energy genes in C2C12 cells. *Mstn* KO resulted in increased expression of related-energy metabolism genes in C2C12 cells. Significant increases in IL-6 and PPAR-γ mRNA expression in response to *Mstn* KO were observed. However, the expression of TNF-α mRNA was decreased (Fig. 5A).

We examined the expression of glucose metabolism-related genes such as Glut1, Glut3, and HEK2 (Fig. 5B). Glut1 and HEK2 were significantly increased in *Mstn* KO C2C12 cells compared with the control group. However, Glut3 was decreased in *Mstn* KO C2C12 cells compared with control group cells. To determine whether increased Glut4 expression was involved in the improved physical endurance associated with *Mstn* KO, we measured the Glut4 protein levels in C2C12 cells. As shown in Fig. 5C, Glut4 protein levels in the *Mstn* KO C2C12 cells were upregulated compared with those in normal control groups, suggesting that Glut4 plays a significant role in the increased physical endurance of *Mstn* KO C2C12 cells. We also found that *Mstn* KO reduced the expression of fatty acid-related genes. Unsaturated fatty acids and fatty acids were mainly synthesised by fatty acid desaturase (Δ-9-desaturase), acetyl-CoA carboxylase (ACC) and fatty acid synthase (FASN). Interestingly, we found a substantial decrease in the gene expression of Δ-9-desaturase (also known as stearoyl-CoA desaturase, SCD) in *Mstn* KO C2C12 cells (Fig. 5D). Moreover, the relative expression of FASN was analysed by Western blotting to determine the C2C12 cell energy metabolism (Fig. 5D). We found that MSTN dysfunction could significantly increase intracellular ATP levels in proliferating C2C12 myoblasts (Fig. 5E) and differentiated C2C12 myotubes after 8 d (Fig. 5F). Taken together, these results demonstrate that MSTN altered the energy metabolism of C2C12 cells energy metabolism by regulating the glucose and lipid metabolism; moreover, the ATP content in *Mstn* KO C2C12 cells was also increased compared with that in wild-type cells.

Next, we further examined the effect of *Mstn* KO on mitochondrial function in C2C12 cells. ΔΨm were determined using JC-1 dye to assess the effect of *Mstn* KO on mitochondrial membrane potential. The *Mstn* KO cells did not show a significant change in ΔΨm (Fig. 6A). Moreover, the *Mstn* KO cells did not display any increase in lactate concentration or glucose uptake compared with those of the wild-type cells (Fig. 6B and Fig. 6C). These results suggest that *Mstn* KO increased the energy metabolism and not damaged health of C2C12 cells.

Fig. 3. Effects of promoting proliferation and mitochondrial biogenesis on *Mstn* KO C2C12 myoblast. (A) Time course of C2C12 myotube proliferation. (B) mRNA expression of KIF5B, PGC-1α and ND1 in the differentiation of C2C12 myotubes. (C) Relative mRNA expression of Cox1, Cox2, ND1 and ND2. (D) Western blot of cell lysates with COX2 and PGC-1α antibodies. β-actin served as a loading control. Numbers 6, 101 and 103 represent different *Mstn* KO cell clones. (E) Relative mitochondrial content was assessed by mitochondrial DNA (mDNA) copies numbers normalised with nuclear DNA (nDNA) copies number in C2C12 cells. WT: wild type; KO: #6 cell clone. $^{*}P < 0.05$; $^{**}P < 0.01$ compared with empty vector control.

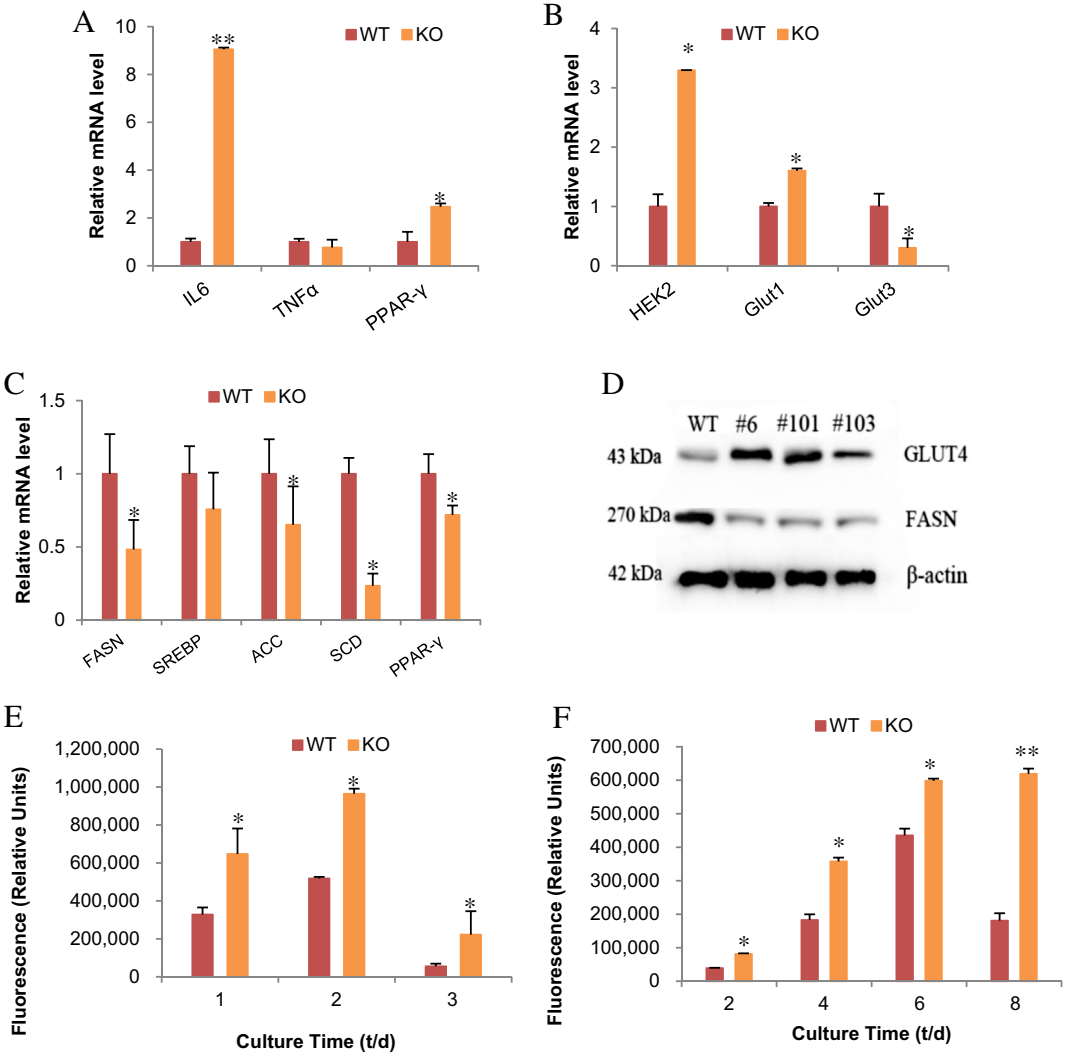

Fig. 5. Knockout of *Mstn* gene regulates mitochondrial energy metabolism. (A) Relative mRNA expression of IL-6, PPAR-γ and TNF-α. (B) Relative mRNA expression of genes associated with skeletal muscle C2C12 cell glucose metabolism. (C) Relative mRNA expression of genes associated with skeletal muscle C2C12 cell lipid metabolism. (D) Western blot analysis of mitochondrial energy metabolism. The relative expression of GLUT4 and FASN were analysed using ImageJ software. Numbers 6, 101 and 103 represent different *Mstn* KO cell clones. Intracellular ATP contents (5E and 5F). WT: wild type; KO: #6 cell clone. $^{*}P < 0.05$; $^{**}P < 0.01$ compared with empty vector control.

4. Discussion

The current study is, to the best of our knowledge, the first to investigate the effect of myostatin on mitochondrion biogenesis and metabolism in the C2C12 myoblast cell line. We demonstrated that myostatin was decreased in *Mstn* KO cells compared to wild-type cells using RT-qPCR and Western blot methods. The KO of this gene promoted cell proliferation, differentiation, mitochondrial biogenesis and energy metabolism without influencing the cells' survival ability.

All kinds of myokines, including cytokines, growth factors, hormones and vasoactive factors were secreted by extremely active endocrine organ, namely skeletal muscle, which have been proposed as the mediators of beneficial biology activity (**Table S3**). Skeletal muscle influences whole-body insulin sensitivity and metabolic homoeostasis. Mitochondrial biogenesis is a prominent adaptation to endurance training in skeletal muscle tissue. Increased mitochondrial density in the muscle fibres contributes to an enhanced aerobic capacity and thereby to improved fatigue resistance [28]. Therefore, we examined whether *Mstn* KO increased mitochondrial biogenesis and influenced the energy metabolism of mitochondria by measuring the mitochondrial content and the expression of energy metabolism-related genes. Myostatin primarily affects mitochondrial biogenesis, and we showed that the mechanism is related to PGC-1α and COX2 expression in C2C12 myoblasts because *Mstn* KO in C2C12 cells led to increased mRNA and protein levels of PGC-1α and COX2. PGC-1α is a transcriptional coactivator that controls mitochondrial oxidative function, enhances mitochondrial biogenesis and inhibits the transcriptional activity of FoxO [29,30]. PGC-1α also prevents the excessive activation of proteolytic systems during muscle atrophy [31]. The overexpression of the PGC1α gene can promote the transformation of glycolytic muscle fibre to oxidative muscle fibre in pigs [32]. Myostatin inhibition and exercise can increase the PGC-1α mRNA level in skeletal muscle. COX, also referred to as complex IV, is the unique terminal oxidase of the mitochondrial respiratory chain (RC) in mammals and consists of thirteen subunits that catalyse the transfer of electrons from ferro-cytochrome *c* to molecular oxygen. This exergonic reaction is coupled to proton transfer across the inner membrane, which contributes to the electrochemical gradient used for ATP synthesis [33]. In this study, in agreement with previous findings, we found that mitochondrial protein and DNA levels were changed in mitochondrial biogenesis [34]. Previous studies reported that *Mstn*-null mice have a lower mitochondrial number [19,35]. However, Camporez et al.'s studies on the $Mstn^{-/-}$ mouse strain and wild-type mice that were treated with antimyostatin antibodies

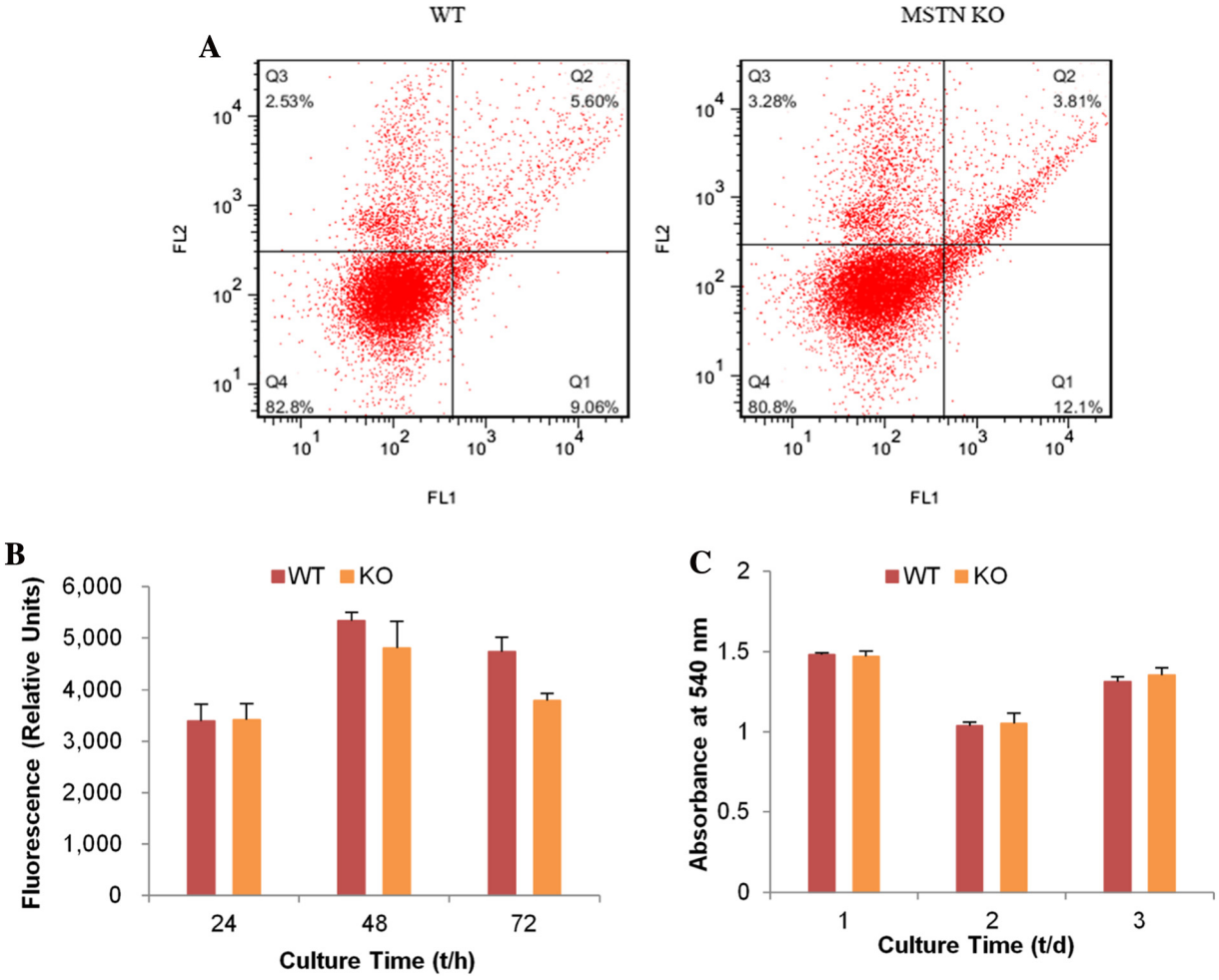

Fig. 6. (A) Mitochondrial membrane potential (ΔΨm). Q1: The cells in this area are early apoptotic cells; Q2: The cells in this area are late apoptotic cells; Q3: The cells in this area are necrotic cells, a small number of late apoptotic cells and even included some mechanical damage cells; Q4: The cells in this area are living cells; (B) Lactate concentration and (C) time course of C2C12 myoblast glucose uptake. WT: wild type; KO: #6 cell clone.

proved an increase in grip strength [36]. These seemingly contradictory results may be because of the limitation of myostatin during different stages (embryonic and adult) or caused by different degrees of inhibition of myostatin skeletal muscle fibres relative to the muscle cell nucleus. In our study, *Mstn* KO promoted mitochondrial biogenesis in C2C12 cells.

Yi et al. [37] found that MSTN disruption could increase the expression of KIF5B mRNA. KIF5B is a heavy chain of the kinesin-1 motor that could interact with BNIP-2. During myogenic differentiation, the KIF5B-dependent anterograde transport of BNIP-2 is critical for its promyogenic effects. We hypothesised that the mechanism by which *Mstn* KO promotes C2C12 cell differentiation is related to KIF5B expression.

Exciting insights into the molecular function of myostatin have been gained. To the best of our knowledge, our study show that the increased proliferation of C2C12 myoblasts produced by *Mstn* KO also alters mitochondrial energy metabolism, regulating the expression of HEK2, Glut1, IL-6, PPAR-γ and TNF-β. As well known, HEK2 is mostly expressed in skeletal muscle and adipose tissues, hexokinase play a key mediator in aerobic glycolysis of glucose metabolism, because the conversion of glucose to glucose 6-phosphate (G-6-P) was catalysed by hexokinase, which is the first rate-limiting step in glucose metabolism [38,39]. Glucose transported through glucose transporters (GLUTs) on the plasma membrane is phosphorylated by HEKs to produce glucose-6-phosphate (G-6-P). Myostatin has been reported to regulate mitochondrial metabolism by promoting glucose consumption and glucose uptake in C2C12 muscle cells [40]. Consistent with our findings, myostatin dysfunction results in increase skeletal muscle mass but impaired force generation [35].

Respiratory metabolism and mitochondrial dynamics was affected by phospholipids [26]. Baati et al. [41] observed SCD1 was decreased in *Mstn*-deficient muscles, concomitant with changes the components of phospholipids. Baati et al. also found that the content of FANS was decreased in *Mstn* KO gastrocnemius compared to the wild type. Zhang et al. [42] observed consistently increased mitochondrial activity and fatty acid oxidation in the skeletal muscle of *Mstn* KO. In line with these previous studies, we have found that expression of genes related to fatty acid oxidation was decreased in *Mstn* KO C2C12 cells. Within this study, we have proved that myostatin regulates fatty acid metabolism in C2C12 cells.

Mitochondria are the main source of mitochondrial reactive oxygen species (mtROS) production, which activates NLRP3 to produce proinflammatory factors [43]. The inflammatory process results from changes in the anabolic and catabolic mediators. The decline in the serum concentrations of anabolic hormones causes muscle catabolism [44]. IL-6 was released into the blood circulation by skeletal muscle fibres in response to muscle contractions [45]. Circulating IL-6 acts as an energy sensor to increase glucose uptake and fatty acid oxidation [46]. TNF-α is a polypeptide cytokine that promotes antitumour and immune responses. TNF-α and interleukin 1 beta (IL-1β) from tumours can interfere with host immunity and skeletal muscle function [47]. TNF-α has been shown to impair the muscle oxidative

phenotype and cause muscle wasting [48]. Our results are in agreement with the findings by Dankbar et al. [49] and Kazemi et al. [50]. A potential consequence of muscle cell hypertrophy is increased anaerobic glycolysis, which could lead to lactic acidaemia. However, *Mstn*$^{-/+}$ KO C2C12 cells did not produce any increase in lactate concentration in cells compared with wild-type cells, consistent with a previous report [50].

Collectively considered, these data provide the compelling evidence that myostatin dysfunction can regulate mitochondrion biogenesis and energy metabolism in C2C12 cells. The data allow us to recognise that MSTN play a vital role in the mitochondrial function suggesting the potential utility of this gene-editing approach for animal breeding and metabolic diseases.

Financial support

This work was supported by grants from the National Natural Science Foundation of China (31772571, 31872332), National Key Research and Development Program (2016YFD0500508, 2018YFD0501905) and the Key Research Program of Shaanxi Province (2017NY-072).

Conflict of interest

The authors declare that they have no competing or financial interests this study.

Supplementary material

https://doi.org/10.1016/j.ejbt.2019.03.009

References

[1] Jinek M, Chylinski K, Fonfara I, et al. A programmable dual-RNA-guided DNA endonuclease in adaptive bacterial immunity. Science 2012;337(6096):816–21. https://doi.org/10.1126/science.1225829 PMid: 22745249.
[2] Hwang WY, Al E. Efficient genome editing in zebrafish using a CRISPR-Cas system. Nat Biotechnol 2013;31(3):227–9. https://doi.org/10.1038/nbt.2501 PMid: 23360964.
[3] Li D, Qiu Z, Shao Y, et al. Heritable gene targeting in the mouse and rat using a CRISPR-Cas system. Nat Biotechnol 2013;31(8):681–3. https://doi.org/10.1038/nbt.2661 PMid: 23929336.
[4] Niu Y, Shen B, Cui Y, et al. Generation of gene-modified cynomolgus monkey via Cas9/RNA-mediated gene targeting in one-cell embryos. Cell 2014;156(4):836–43. https://doi.org/10.1016/j.cell.2014.01.027 PMid: 24486104.
[5] Hai T, Teng F, Guo R, et al. One-step generation of knockout pigs by zygote injection of CRISPR/Cas system. Cell Res 2014;24(3):372–5. https://doi.org/10.1038/cr.2014.11 PMid: 24481528.
[6] Wang X, Yu H, Lei A, et al. Generation of gene-modified goats targeting MSTN and FGF5 via zygote injection of CRISPR/Cas9 system. Sci Rep 2015;5:13878. https://doi.org/10.1038/srep13878 PMid: 26354037.
[7] Mcpherron AC, Lawler AM, Lee S. Regulation of skeletal muscle mass in mice by a new TGF-beta superfamily member. Nature 1997;387(6628):83–90. https://doi.org/10.1038/387083a0 PMid: 9139826.
[8] Kambadur R, Sharma M, Smith TPL, et al. Mutations in myostatin (GDF8) in double-muscled Belgian blue and Piedmontese cattle. Genome Res 1997;7(9):910–5. https://doi.org/10.1101/gr.7.9.910 PMid: 9314496.
[9] Lee HC, Lim ML, Lu CY, et al. Concurrent increase of oxidative DNA damage and lipid peroxidation together with mitochondrial DNA mutation in human lung tissues during aging–smoking enhances oxidative stress on the aged tissues. Arch Biochem Biophys 1999;362(2):309–16. https://doi.org/10.1006/abbi.1998.1036 PMID: 9989940.
[10] Wallace DC. Mitochondrial DNA variation in human radiation and disease. Cell 2015;163(1):33–8. https://doi.org/10.1016/j.cell.2015.08.067 PMid: 26406369.
[11] Demers-Lamarche J, Guillebaud G, Tlili M, et al. Loss of mitochondrial function impairs lysosomes. J Biol Chem 2016;291(19):10263–76. https://doi.org/10.1074/jbc.m115.695825 PMID: 26987902.
[12] Rich P. Chemiosmotic coupling: the cost of living. Nature 2003;421(6923):583. https://doi.org/10.1038/421583a PMid: 12571574.
[13] Franzini-Armstrong C, Jorgensen AO. Structure and development of EC coupling units in skeletal muscle. Annu Rev Physiol 1994;56(1):509–34. https://doi.org/10.1146/annurev.ph.56.030194.002453 PMid: 8010750.
[14] Russell AP, Foletta VC, Snow RJ, et al. Skeletal muscle mitochondria: a major player in exercise, health and disease. Biochim Biophys Acta Gen Subj 2014;1840(4):1276–84. https://doi.org/10.1016/j.bbagen.2013.11.016 PMid: 24291686.
[15] Huang JH, Hood DA. Age-associated mitochondrial dysfunction in skeletal muscle: contributing factors and suggestions for long-term interventions. IUBMB Life 2009;61(3):201–14. https://doi.org/10.1002/iub.164 PMid: 19243006.
[16] Angelin A, Tiepolo T, Sabatelli P, et al. Mitochondrial dysfunction in the pathogenesis of Ullrich congenital muscular dystrophy and prospective therapy with cyclosporins. Proc Natl Acad Sci U S A 2007;104(3):991–6. https://doi.org/10.1073/pnas.0610270104 PMid: 17215366.
[17] Irwin WA, Bergamin N, Sabatelli P, et al. Mitochondrial dysfunction and apoptosis in myopathic mice with collagen VI deficiency. Nat Genet Nat Genet 2003;35(4):367–71. https://doi.org/10.1038/ng1270 PMid: 14625552.
[18] Antunes D, Padrao AI, Maciel E, et al. Molecular insights into mitochondrial dysfunction in cancer-related muscle wasting. Biochim Biophys Acta 2014;1841(6):896–905. https://doi.org/10.1016/j.bbalip.2014.03.004 PMid: 24657703.
[19] Ploquin C, Chabi B, Fouret G, et al. Lack of myostatin alters intermyofibrillar mitochondria activity, unbalances redox status, and impairs tolerance to chronic repetitive contractions in muscle. Am J Physiol Endocrinol Metab 2012;302(8). https://doi.org/10.1152/ajpendo.00652.2011 PMid: 22318951.
[20] Girgenrath S, Song K, Whittemore LA. Loss of myostatin expression alters fiber-type distribution and expression of myosin heavy chain isoforms in slow- and fast-type skeletal muscle. Muscle Nerve 2005;31(1):34–40. https://doi.org/10.1002/mus.20175 PMid: 15468312.
[21] Rooney MF, Porter RK, Katz LM, et al. Skeletal muscle mitochondrial bioenergetics and associations with myostatin genotypes in the thoroughbred horse. PLoS One 2017;12(11):e0186247. https://doi.org/10.1371/journal.pone.0186247 PMid: 29190290.
[22] Wang L, Cai B, Zhou S, et al. RNA-seq reveals transcriptome changes in goats following myostatin gene knockout. PLoS One 2017;12(12):e0187966. https://doi.org/10.1371/journal.pone.0187966 PMid:29228005.
[23] Puddick J, Martinus RD. Comparative proteomics of skeletal muscle mitochondria from myostatin-null mice. Cell Biol Int Rep 2011;18(2):35–41. https://doi.org/10.1042/cbr20110006 PMID: 23124711.
[24] Shen B, Zhang J, Wu H, et al. Generation of gene-modified mice via Cas9/RNA-mediated gene targeting. Cell Res 2013;23(5):720–3. https://doi.org/10.1038/cr.2013.46 PMid: 23545779.
[25] Zhou X, Li R, Liu X, et al. ROCK1 reduces mitochondrial content and irisin production in muscle suppressing adipocyte browning and impairing insulin sensitivity. Sci Rep 2016;6(1):29669. https://doi.org/10.1038/srep29669 PMID: 27411515.
[26] Mårtensson CU, Doan KN, Becker T. Effects of lipids on mitochondrial functions. Biochim Biophys Acta 2017;1862(1):102–13. https://doi.org/10.1016/j.bbalip.2016.06.015 PMid: 27349299.
[27] McPherron AC, Lee SJ. Double muscling in cattle due to mutations in the myostatin gene. Proc Natl Acad Sci U S A 1997;94(23):12457–61. https://doi.org/10.1073/pnas.94.23.12457 PMid: 9356471.
[28] Hood DA, Chabi B, Menzies K. Exercise-induced mitochondrial biogenesis in skeletal muscle. Milan: Springer; 2007.
[29] Peterson CM, Johannsen DL, Ravussin E. Skeletal muscle mitochondria and aging: a review. J Aging Res 2012;2012:194821. https://doi.org/10.1155/2012/194821 PMID: 22888430.
[30] Han HQ, Zhou X, Mitch WE, et al. Myostatin/activin pathway antagonism: molecular basis and therapeutic potential. Int J Biochem Cell Biol 2013;45(10):2333–47. https://doi.org/10.1016/j.biocel.2013.05.019 PMid: 23721881.
[31] Vainshtein A, Desjardins EMA, Armani A, et al. PGC-1α modulates denervation-induced mitophagy in skeletal muscle. Skelet Muscle 2015;5(1):9. https://doi.org/10.1186/s13395-015-0033-y PMid: 25834726.
[32] Ying F, Zhang L, Bu G, et al. Muscle fiber-type conversion in the transgenic pigs with overexpression of PGC1alpha gene in muscle. Biochem Biophys Res Commun 2016;480(4):669–74. https://doi.org/10.1016/j.bbrc.2016.10.113 PMid: 27983980.
[33] Rak M, Bénit P, Chrétien D, et al. Mitochondrial cytochrome *c* oxidase deficiency. Clin Sci 2016;130(6):393. https://doi.org/10.1042/CS20150707 PMid: 26846578.
[34] Liang H, Bai Y, Li Y, et al. PGC-1α-induced mitochondrial alterations in 3T3 fibroblast cells. Ann N Y Acad Sci 2007;1100(1):264–79. https://doi.org/10.1196/annals.1395.028 PMid: 17460188.
[35] Amthor H, Macharia R, Navarrete R, et al. Lack of myostatin results in excessive muscle growth but impaired force generation. Proc Natl Acad Sci U S A 2007;104(6):1835–40. https://doi.org/10.1073/pnas.0604893104 PMid: 17267614.
[36] Camporez JG, Petersen MC, Abudukadier A, et al. Anti-myostatin antibody increases muscle mass and strength and improves insulin sensitivity in old mice. Proc Natl Acad Sci U S A 2016;113(8):2212–7. https://doi.org/10.1073/pnas.1525795113 PMid: 26858428.
[37] Yi P, Chew LL, Zhang Z, et al. KIF5B transports BNIP-2 to regulate p38 mitogen-activated protein kinase activation and myoblast differentiation. Mol Biol Cell 2015;26(1):29–42. https://doi.org/10.1091/mbc.e14-03-0797 PMid: 25378581.
[38] Liu Y, Cheng H, Zhou Y, et al. Myostatin induces mitochondrial metabolic alteration and typical apoptosis in cancer cells. Cell Death Dis 2013;4(2):e494. https://doi.org/10.1038/cddis.2013.31 PMid: 23412387.
[39] John S, Weiss JN, Ribalet B. Subcellular localization of hexokinases I and II directs the metabolic fate of glucose. Plos One 2011;6(3):e17674. https://doi.org/10.1371/journal.pone.0017674 PMid: 21408025.
[40] Chen Y, Ye J, Cao L, et al. Myostatin regulates glucose metabolism via the AMP-activated protein kinase pathway in skeletal muscle cells. Int J Biochem Cell Biol 2010;42(12):2072–81. https://doi.org/10.1016/j.biocel.2010.09.017 PMid: 20887798.

[41] Baati N, Feillet-Coudray C, Fouret G, et al. Myostatin deficiency is associated with lipidomic abnormalities in skeletal muscles. Biochim Biophys Acta 2017;1862 (10):1044–55. Pt. A. https://doi.org/10.1016/j.bbalip.2017.06.017 PMid: 28676454.
[42] Zhang C, McFarlane C, Lokireddy S, et al. Inhibition of myostatin protects against diet-induced obesity by enhancing fatty acid oxidation and promoting a brown adipose phenotype in mice. Diabetologia 2012;55(1):183–93. https://doi.org/10.1007/s00125-011-2304-4 PMid: 21927895.
[43] Zhou R, Yazdi AS, Menu P, et al. A role for mitochondria in NLRP3 inflammasome activation. Nature 2011;469(7329):221. https://doi.org/10.1038/nature09663 PMid: 21124315.
[44] Margutti KMDM, Schuch NJ, Schwanke CHA. Inflammatory markers, sarcopenia and its diagnostic criteria among the elderly: a systematic review. 2017;20(3):441–53. https://doi.org/10.1590/1981-22562017020.160155.
[45] Steensberg A, van Hall G, Osada T, et al. Production of interleukin-6 in contracting human skeletal muscles can account for the exercise-induced increase in plasma interleukin-6. J Physiol 2000;529(Pt 1):237–42. https://doi.org/10.1111/j.1469-7793.2000.00237.x PMid: 11080265.
[46] Carey AL, Steinberg GR, Macaulay SL, et al. Interleukin-6 increases insulin-stimulated glucose disposal in humans and glucose uptake and fatty acid oxidation in vitro via AMP-activated protein kinase. Diabetes 2006;55(10):2688–97. https://doi.org/10.2337/db05-1404 PMid: 17003332.
[47] Wang X, Gao X, Xu Y. MAGED1: molecular insights and clinical implications. Ann Med 2011;43(5):347–55. https://doi.org/10.3109/07853890.2011.573806 PMid: 21612333.
[48] Remels AH, Gosker HR, Schrauwen P, et al. TNF-alpha impairs regulation of muscle oxidative phenotype: implications for cachexia? FASEB J 2010;24(12):5052–62. https://doi.org/10.1096/fj.09-150714 PMid: 20807714.
[49] Dankbar B, Fennen M, Brunert D, et al. Myostatin is a direct regulator of osteoclast differentiation and its inhibition reduces inflammatory joint destruction in mice. Nat Med 2015;21(9):1085–90. https://doi.org/10.1038/nm.3917 PMid: 26236992.
[50] Kazemi F. The correlation of resistance exercise-induced myostatin with insulin resistance and plasma cytokines in healthy young men. J Endocrinol Invest 2016; 39(4):383–8. https://doi.org/10.1007/s40618-015-0373-9 PMid: 26280319.